ELSEVIER

Chemical Physics 266 (2001) 311–322

Chemical Physics

www.elsevier.nl/locate/chemphys

Two-dimensional correlation spectroscopies of localized vibrations

Andrei Piryatinski [1], Vladimir Chernyak [2], Shaul Mukamel *

Department of Chemistry, Rochester Theory Center for Optical Science and Engineering, University of Rochester, P.O. RC Box 270216, Rochester, NY 14627-0216, USA

Received 29 November 2000

Abstract

One- and two-dimensional vibrational response functions which may be used in the simulations of molecular fifth-order Raman and second-order infrared techniques are calculated for a set of interacting localized anharmonic vibrations. Employing a vibrational Frenkel exciton model we have accounted for exciton–exciton scattering due to quartic anharmonicities as well as for the creation and annihilation of one vibrational quanta by cubic anharmonicities. Closed expressions for the optical response are given in terms of the one- and two-exciton Green functions, the exciton scattering matrix and the exciton population Green function.

1. Introduction

Multiple-pulse coherent techniques using ultrashort ($\geqslant 10$ fs) optical pulses provide a wealth of information about vibrational motions and relaxation processes. The signal can be represented in the time domain as a multidimensional function of the various delay times, or in analogy with the multidimensional NMR spectroscopies [1–3], as the Fourier transform in the frequency domain.

A coherent Raman experiment involves the application of n pairs of electronically off-resonant pulses which generate and control vibrational coherence in the ground electronic state, followed by a final detection pulse which is scattered off the sample (Fig. 1(A)) [4]. The $(2n+1)$th order response to this sequence of $2n+1$ pulses has n controlled delay times and constitutes an n-dimensional (nD) spectroscopy. Resonant multidimensional infrared (IR) techniques provide an alternative to off-resonant multidimensional Raman spectroscopies. An nD IR experiment employs a train of n phase-locked IR pulses (Fig. 1(B)). Using heterodyne detection of the nth order polarization created by the pulse sequence, there are n delay times which can be experimentally controlled. The nth order response thus constitutes an nD signal as well.

In this article we focus on 2D techniques. For clarity we discuss the fifth-order Raman. However, all the results can be used directly to compute the second-order IR signals, making use of the exact formal correspondence between the $(2n+1)$-order

* Corresponding author. Tel.: +1-716-275-3080; fax: +1-716-473-6889.

E-mail address: mukamel@chem.rochester.edu (S. Mukamel).

[1] Present address: Department of Chemistry, University of Wisconsin, Madison, WI 53706, USA.

[2] Present address: Corning Incorporated, Process Engineering and Modeling, Corning, NY 14831, USA.

0301-0104/01/$ - see front matter
PII: S0301-0104(01)00253-1

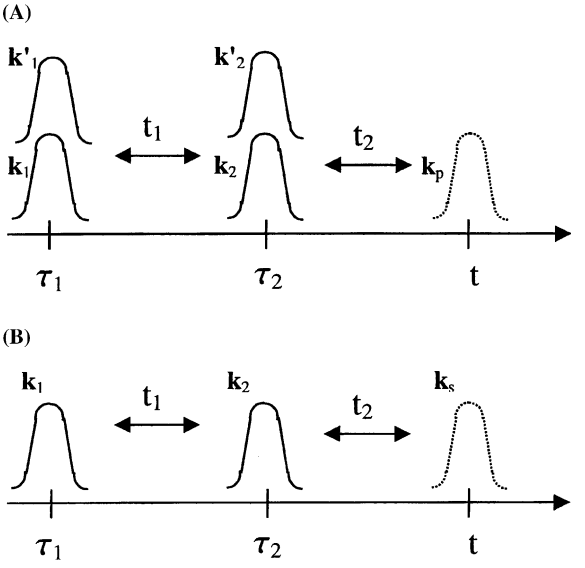

Fig. 1. Pulse sequences in two-dimensional techniques. (A) Fifth-order Raman experiment. The signal shows up in the directions $\mathbf{k}_p = \pm(\mathbf{k}_1 - \mathbf{k}_1') \pm (\mathbf{k}_2 - \mathbf{k}_2') \pm \mathbf{k}_3$. (B) Second-order IR. The signal shows up in the directions $\mathbf{k}_s = \pm\mathbf{k}_1 \pm \mathbf{k}_2$.

off-resonance Raman and nth order IR [4]: the nD signals are given by $n+1$ time correlation functions of the polarizability (Raman) and the dipole operator (IR).

The fifth-order off-resonant Raman technique proposed by Tanimura and Mukamel [5], (Fig. 1(A)) is now the focus of intensive experimental and theoretical studies. 2D Raman measurements are primarily oriented towards the investigation of the inter and intramolecular vibrational dynamics of simple liquids (e.g. CS_2) [6–25]. The capacity of this technique to separate homogeneous and inhomogeneous broadening has been demonstrated in Ref. [5]. It further provides the complete set of relaxation parameters (i.e. inhomogeneous dephasing time, population decay and pure dephasing) [26,27]. Assuming dipole–dipole interaction between two harmonic oscillators with nonlinear polarizability, Okumura, Tokmakoff, and Tanimura, have studied the cross-peak intensity scaling with the distance between the dipoles [25]. This demonstrates the ability of 2D Raman techniques to provide structural information by extracting the distances between the dipoles.

The theoretical treatment of 2D Raman experiments is based on the normal mode analysis of coupled anharmonic molecular vibrations. Applying the Born–Oppenheimer approximation, the electronic polarizability and the Hamiltonian are averaged over the ground electronic state and considered as operators which depend nonlinearly on the normal mode coordinates [28]. The necessary $n+1$ point correlation functions of the electronic polarizability were calculated by Khidekel and Mukamel using the coherent state representation. They derived expressions for the third-, fifth- and seventh-order response functions of a single harmonic oscillator whose electronic polarizability depends exponentially on the primary vibrational coordinate [29]. Two types of semiclassical approximations were proposed to model the vibrational dynamics of the nonlinear response functions: a high temperature algorithm [30] and a weak anharmonicity expansion [31–34]. The high temperature algorithm was used by Williams and Loring to calculate classical infrared photon echoes in liquids [35]. Both approximations were compared in Refs. [32–34] using the Brownian oscillator model as well as the wave-packet representation of the quantum model. Multiple echoes were predicted for the harmonic oscillator with nonlinear electronic polarizability. Using the instantaneous normal mode approach, Saito and Ohmine have performed classical simulations of the Raman echoes in liquid water and CS_2 and demonstrated the effect of Raman echo reduction due to intermode mixing [36].

When the vibrational frequencies Ω_n are higher than thermal energy k_BT, the third- and the fifth-order response functions $R^{(3)}(t;\tau_1)$ and $R^{(5)}(t,\tau_1,\tau_2)$ introduced in Refs. [32–34] only involve the ground, single- and double-excited vibrational states. The 2D third-order nonlinear response of Frenkel excitons depends on the one- and two-exciton manifolds [37] and can be expressed in terms of one-exciton Green function, exciton scattering matrix and the exciton population Green functions. For linear coupling between the excitons and harmonic (bath) degrees of freedom, these quantities satisfy a closed set of equations for the one-exciton, one–two-exciton coherences and exciton density matrix, respec-

tively, derived in Ref. [38] and referred as the nonlinear exciton equations (NEE). Closed expressions for the 2D signal ($R^{(7)}$ Raman response) were obtained in Ref. [39] by solving the NEE. $R^{(5)}$ vanishes for that model. Application of 2D Raman techniques to study collective dynamics of localized vibrations, such as the amide I vibrations in proteins and polypeptides [40] requires the generalization of the vibrational Frenkel exciton model used in Refs. [41–45]. In this article we extend the model to include higher anharmonicities and quadratic dependence of the polarizability which allow us to calculate $R^{(5)}$ as well.

2. 2D response of vibrational excitons

We consider a system of coupled localized anharmonic vibrations described by the Hamiltonian

$$H = H_0 + H_1, \tag{2.1}$$

$$H_0 = \frac{1}{2}\sum_{mn}\left[\delta_{mn}\left(\frac{P_m^2}{2M_m} + \Omega_m^{(0)^2} M_m Q_m^2\right) + (1-\delta_{mn})U_{mn}^{(2)} Q_m Q_n\right], \tag{2.2}$$

$$H_1 = \frac{1}{3!}\sum_{mnk} U_{mnl}^{(3)} Q_m Q_n Q_l + \frac{1}{4!}\sum_{mn,lk} U_{mn,lk}^{(4)} Q_m Q_n Q_l Q_k, \tag{2.3}$$

where P_m and Q_m are the momentum and coordinate of the mth vibration with mass M_m. H_0 represents the harmonic part. Its first (diagonal) term, describes normal local oscillators with frequency $\Omega_n^{(0)}$ whereas $U^{(2)}$ represents harmonic couplings. $U^{(3)}$ and $U^{(4)}$ are anharmonic couplings among vibrations.

To compute the optical response we first express the vibrational coordinates in terms of the creation (annihilation) operators $\hat{B}_m(\hat{B}_m^\dagger)$

$$Q_m = \frac{1}{\sqrt{2M_m\Omega_m^{(0)}}}(\hat{B}_m^\dagger + \hat{B}_m), \qquad P_m = i\sqrt{M_m\Omega_m^{(0)}/2}\,(\hat{B}_m^\dagger - \hat{B}_m), \tag{2.4}$$

with the Bose commutation relations:

$$[\hat{B}_n, \hat{B}_m^\dagger] = \delta_{nm}. \tag{2.5}$$

Substituting Eq. (2.4) into Eqs. (2.1)–(2.3), retaining only those terms which either conserve the number of vibrational quanta or create and annihilate a single vibrational quantum, results in the vibrational Hamiltonian

$$\hat{H} = \sum_{mn} h_{mn}\hat{B}_m^\dagger \hat{B}_n + \sum_{mnk} V_{mnk}^{(3)}(\hat{B}_m^\dagger \hat{B}_n^\dagger \hat{B}_k + \hat{B}_m^\dagger \hat{B}_n \hat{B}_k) + \sum_{mnkl} V_{mn,kl}^{(4)} \hat{B}_m^\dagger \hat{B}_n^\dagger \hat{B}_k \hat{B}_l, \tag{2.6}$$

where

$$h_{mn} = \delta_{mn}\Omega_n + (1-\delta_{mn})J_{mn}, \tag{2.7}$$

$$\Omega_m = \Omega_m^{(0)} + \frac{1}{2}\sum_l V_{mm,ll}^{(4)}, \tag{2.8}$$

$$J_{mn} = \frac{1}{2}\sum_{mn}\frac{U_{mn}^{(2)}}{\sqrt{M_m M_n \Omega_m^{(0)}\Omega_n^{(0)}}} + \frac{1}{2}\sum_l V_{mn,ll}^{(4)}$$

and

$$V_{mnl}^{(3)} = \frac{1}{2\times 3!}\sum_{\text{perm}}\frac{U_{mnl}^{(2)}}{\sqrt{M_m M_n M_l \Omega_m^{(0)}\Omega_n^{(0)}\Omega_l^{(0)}}}, \tag{2.9}$$

$$V_{mn,lk}^{(4)} = \frac{1}{2\times 4!}\times\sum_{\text{perm}}\frac{U_{mn,lk}^{(4)}}{\sqrt{M_m M_n M_k M_l \Omega_m^{(0)}\Omega_n^{(0)}\Omega_k^{(0)}\Omega_l^{(0)}}}. \tag{2.10}$$

The summations in Eqs. (2.9) and (2.10) run over all permutations of the indices, corresponding to symmetrized energy terms. The collective vibrational modes described by the linearized first term of Eq. (2.6) are denoted vibrational excitons, and Eq. (2.6) is the vibrational-exciton Hamiltonian.

The total Hamiltonian which includes the coupling with the radiation field has the form [28]

$$\hat{H}_T = \hat{H} - \mathscr{E}^2(t)\hat{\alpha}, \tag{2.11}$$

where $\hat{\alpha}$ is the electronic polarizability, averaged over the electronic ground state, which depends on

vibrational coordinates. [3] The radiation field $\mathscr{E}(t)$ consists of two pairs of ultra-short nonoverlapping pulses $\mathscr{E}_j$, $j=1$, 2, centered at times τ_1 and τ_2, $(\tau_1>\tau_2)$, followed by the probe pulse $\mathscr{E}_{\rm p}(t-\tau_{\rm p})$ centered at $\tau_{\rm p}$ (Fig. 1(A)):

$$\mathscr{E}(t)=\sum_{j=1}^{2}\mathscr{E}_j(t-\tau_j)+\mathscr{E}_{\rm p}(t-\tau_{\rm p}). \tag{2.12}$$

We further expand the electronic polarizability to second order in the oscillator operators:

$$\hat{\alpha}=\sum_n(\mu_n^{(1)}\hat{B}_n+\mu_n^{(1)^*}\hat{B}_n^\dagger)+\sum_{mn}(\mu_{mn}^{(2)}\hat{B}_m\hat{B}_n+\mu_{mn}^{(2)^*}\hat{B}_m^\dagger\hat{B}_n^\dagger)+d_{mn}\hat{B}_m^\dagger\hat{B}_n, \tag{2.13}$$

where $\mu_n^{(1)}$, $\mu_{mn}^{(2)}$, and d_{mn} are expansion coefficients.

The Hamiltonian equation (2.6) with $V^{(3)}=0$ is equivalent to the Hamiltonian previously used to describe electronic Frenkel excitons in molecular aggregates [37,38]. The Heisenberg equation of motion for the vibrational operators $\mathrm{i}\mathrm{d}\hat{B}_m/\mathrm{d}t=[\hat{B}_m,\hat{H}_{\rm T}]$ reads

$$\begin{aligned}\mathrm{i}\frac{\mathrm{d}\hat{B}_m}{\mathrm{d}t}-\sum_n h_{mn}\hat{B}_n=&\sum_{nk}V_{mnk}^{(3)}(\hat{B}_n\hat{B}_k+2\hat{B}_n^\dagger\hat{B}_k)\\&+\sum_{nkl}V_{mn,kl}^{(4)}\hat{B}_n^\dagger\hat{B}_k\hat{B}_l-\mathscr{E}^2(t)\mu_m^{(1)^*}\\&-2\mathscr{E}^2(t)\sum_n\mu_{mn}^{(2)^*}\hat{B}_n^\dagger\\&-\mathscr{E}^2(t)\sum_n d_{mn}\hat{B}_n\end{aligned} \tag{2.14}$$

it can be used to derive a closed system of equations for the variables [38]

$$B_m\equiv\langle\hat{B}_m\rangle,\qquad Y_{mn}\equiv\langle\hat{B}_m\hat{B}_n\rangle,$$
$$N_{ij}\equiv\langle\hat{B}_i^\dagger\hat{B}_j\rangle,\qquad Z_{mn,j}\equiv\langle\hat{B}_j^\dagger\hat{B}_m\hat{B}_n\rangle. \tag{2.15}$$

We further recast the exciton density matrix as $N_{ij}=\langle\hat{B}_i^\dagger\hat{B}_j\rangle^i+\langle\hat{B}_i^\dagger\rangle\langle\hat{B}_j\rangle$, where the second term represents coherent dynamics of the exciton population and the first accounts for bath correlations leading to the pure dephasing and population transport with the one-exciton manifold. In this section we assume coherent population dynamics and retain only the second term in the expression for N_{ij}. An additional contribution to the response function due to the second irreducible term is given in Appendix C. Neglecting pure dephasing between the first and second exciton states, the factorization $Z_{mn,j}=\langle B_j^\dagger\rangle\langle B_mB_n\rangle$ is adopted as well.

Expanding the variables B_n and Y_{mn} in powers of $\mathscr{E}^2(t)$ we obtain the closed system of equations:

$$\mathrm{i}\frac{\mathrm{d}B_m^{(1)}}{\mathrm{d}t}-\sum_n h_{mn}\hat{B}_n^{(1)}-\sum_{nk}V_{mnk}^{(3)}Y_{nk}^{(1)}=-\mathscr{E}^2(t)\mu_m^{(1)^*}, \tag{2.16}$$

$$\mathrm{i}\frac{\mathrm{d}Y_{mn}^{(1)}}{\mathrm{d}t}-\sum_{kl}h_{mn,kl}^{(2)}Y_{kl}^{(1)}-\sum_k V_{mnk}^{(3)}B_k^{(1)}=-2\mathscr{E}^2(t)\mu_{mn}^{(2)^*}, \tag{2.17}$$

$$\begin{aligned}\mathrm{i}\frac{\mathrm{d}B_m^{(2)}}{\mathrm{d}t}-\sum_n h_{mn}\hat{B}_n^{(2)}-\sum_{nk}V_{mnk}^{(3)}Y_{nk}^{(2)}&=-\sum_{nk}V_{mnk}^{(3)}B_n^{(1)^*}B_k^{(1)}+\sum_{nkl}V_{mn,kl}Y_{kl}^{(1)}B_n^{(1)}\\&\quad-2\mathscr{E}^2(t)\sum_n\mu_{mn}^{(2)^*}B_n^{(1)^*}-\mathscr{E}^2(t)\sum_j d_{mj}B_j^{(1)},\end{aligned} \tag{2.18}$$

$$\begin{aligned}\mathrm{i}\frac{\mathrm{d}Y_{mn}^{(2)}}{\mathrm{d}t}-\sum_{kl}h_{mn,kl}^{(2)}Y_{kl}^{(2)}-\sum_k V_{mnk}^{(3)}B_k^{(2)}&=\sum_{skl}V_{skl}^{(3)}(\delta_{sm}\delta_{pn}+\delta_{sn}\delta_{pm})B_k^{(1)^*}Y_{lp}^{(1)}\\&\quad-\mathscr{E}^2(t)(\mu_m^{(1)^*}B_n^{(1)}+\mu_n^{(1)^*}B_m^{(1)})-\mathscr{E}^2(t)\\&\quad\times\sum_{kl}(d_{mk}\delta_{nl}+\delta_{mk}d_{nl})Y_{kl}^{(1)},\end{aligned} \tag{2.19}$$

where $h_{mn,kl}^{(2)}=\delta_{mk}h_{nl}+h_{mk}\delta_{nl}+V_{mn,kl}^{(4)}$ are matrix elements of two-particle Hamiltonian introduced in Refs. [38,46].

The free evolution of the variables B and Y (i.e. when the field is switched off) is given by Eqs. (2.16)–(2.19), with the right-hand side set to zero. It can be represented by the Green functions $G_{mn}^{(B)}$ and $G_{mn,pq}^{(Y)}$ of Eqs. (2.16) and (2.17) defined as

[3] To account for the coupling in the case of IR resonant spectroscopy, the second term in Eq. (2.11), needs to be replaced with $\mathscr{E}(t)\mu$, where μ is vibrational transition dipole in the ground electronic state.

$B_m(t)=\sum_n G^{(B)}_{mn}(t)B_n(0)$ and $Y_{mn}(t)=\sum_{kl} G^{(Y)}_{mn,kl}(t)\times Y_{kl}(0)$. These Green functions also determine free propagation of the dynamical variables in Eqs. (2.18) and (2.19). Elimination of Y from Eqs. (2.16) and (2.18) and of B from Eqs. (2.17) and (2.19) corresponds to the one- and two-exciton states energy renormalization due to the creation and annihilation of virtual two- and one-exciton states. The one-exciton Green function satisfies the Dyson equation.

$$G^{(B)}_{mn}(t)=G^{(B_0)}_{mn}(t)+\sum_{pq}\int \mathrm{d}\tau'\int \mathrm{d}\tau'' \times G^{(B_0)}_{mp}(t-\tau')V^{\mathrm{eff}}_{pq}(\tau'-\tau'')G^{(B)}_{qn}(\tau''), \tag{2.20}$$

where $G^{(B_0)}_{mn}(t)=\theta(t)[\exp(\mathrm{i}ht)]_{mn}$ is one-exciton Green function of Eqs. (2.16) and (2.18) with $V^{(3)}=0$, and effective scattering potential is

$$V^{\mathrm{eff}}_{mn}(\tau)=-2\sum_{pq,kl} V^{(3)}_{mpq}G^{(Y_0)}_{pq,kl}(\tau)V^{(3)}_{kln}. \tag{2.21}$$

In Eq. (2.21) $G^{(Y_0)}_{pq,kl}$ is two-exciton Green function of Eqs. (2.17) and (2.19) with $V^{(3)}=0$, which is determined by the equation

$$G^{(Y_0)}_{mn,pq}(t)=G^{(B_0)}_{mp}(t)G^{(B_0)}_{nq}(t)+\sum_{kl,rs}\int \mathrm{d}\tau'\int \mathrm{d}\tau'' \times G^{(B_0)}_{mk}(t-\tau')G^{(B_0)}_{nl}(t-\tau') \times \bar{\Gamma}_{kl,rs}(\tau'-\tau'')G^{(B_0)}_{rp}(\tau'')G^{(B_0)}_{sq}(\tau''). \tag{2.22}$$

The two-particle scattering matrix can be obtained as the solution of the equation

$$\bar{\Gamma}_{ij,kl}(t)=V^{(4)}_{ij,kl}\delta(t)+\sum_{pq,p'q'}V^{(4)}_{ij,pq}\int_0^t \mathrm{d}\tau' \times G^{(B_0)}_{pp'}(t-\tau')G^{(B_0)}_{qq'}(t-\tau')\bar{\Gamma}_{p'q',kl}(\tau'). \tag{2.23}$$

The Green function $G^{(Y)}$ is determined by the Bethe–Salpeter equation:

$$G^{(Y)}_{mn,kl}(t)=G^{(Y_0)}_{mn,kl}(t)+\sum_{pq,rs}\int \mathrm{d}\tau'\int \mathrm{d}\tau'' \times G^{(Y_0)}_{mn,pq}(t-\tau')U^{\mathrm{eff}}_{pq,rs}(\tau'-\tau'')G^{(Y)}_{rs,kl}(\tau''), \tag{2.24}$$

with

$$U^{\mathrm{eff}}_{mn,kl}(\tau)=-2\sum_{pq}V^{(3)}_{mnp}G^{(B_0)}_{pq}(\tau)V^{(3)}_{qkl}. \tag{2.25}$$

As a consequence of the exciton energy renormalization in Eqs. (2.20) and (2.21), the Green function $G^{(B)}(\omega)$ has two types of resonances, with energies close to the resonances of $G^{(B_0)}(\omega)$ (one exciton) and $G^{(Y_0)}(\omega)$ (two exciton). One- and two-exciton resonances also appear in $G^{(Y)}$, as can be seen from Eqs. (2.24) and (2.25).

The solution of Eqs. (2.16) and (2.17) can be readily given in terms of $G^{(B)}$ and $G^{(Y)}(\omega)$. The third-order response function is

$$P^{(3)}(t)=\int \mathrm{d}\tau_1 R^{(3)}(t;\tau_1)\mathscr{E}^2(t-\tau_1)\mathscr{E}(t), \tag{2.26}$$

with

$$R^{(3)}(t;\tau_1)=\sum_{\alpha=1,2}R^{(3)}_{\alpha}(t;\tau_1), \tag{2.27}$$

and

$$R^{(3)}_1(t;\tau_1)=\sum_{mn}\mu^{(1)}_m\mu^{(1)^*}_n G^{(B)}_{mn}(t-\tau_1), \tag{2.28}$$

$$R^{(3)}_2(t;\tau_1)=\sum_{mn,kl}\mu^{(2)}_{mn}\mu^{(2)^*}_{kl} G^{(Y)}_{mn,kl}(t-\tau_1). \tag{2.29}$$

The fifth-order solution of Eqs. (2.16)–(2.19) can be conveniently represented in terms of the single-particle Green function $G^{(B)}_{mn}(t)$, two-exciton Green function $G^{(Y)}$ and the two-particle scattering matrix $\bar{\Gamma}_{mn,kl}(t)$. This yields

$$P^{(5)}(t)=\int \mathrm{d}\tau_1\int \mathrm{d}\tau_1 R^{(5)}(t;\tau_1,\tau_2) \times \mathscr{E}^2(t-\tau_1-\tau_2)\mathscr{E}^2(t-\tau_2)\mathscr{E}(t), \tag{2.30}$$

with the response function

$$R^{(5)}(t;\tau_2,\tau_1)=\sum_{\alpha=1}^{9}R_{\alpha}(t;\tau_2,\tau_1)+\mathrm{c.c.} \tag{2.31}$$

When $V^{(3)} = 0$ the response function has only the five terms given in Appendix A. When $V^{(3)}$ is included, the response function has seven terms, listed in Appendix B. When the vibrations are coupled to a bath which induces dephasing and relaxation there are two additional contributions (R_8 and R_9), given in Appendix C.

The exciton dynamics contributing to the response function is depicted by the Feynman diagrams shown in Fig. 2. Diagram (1) and (2) in panel (A) show one- and two-exciton propagation giving rise to $R_1^{(3)}$ and $R_2^{(3)}$, respectively. Diagrams (1)–(9) in panel (B) correspond to $R_1^{(5)}$–$R_9^{(5)}$ respectively. Note that diagrams (1) and (2) only involve one-exciton processes, and diagrams (3)–(5) contain various combination of one- and two-exciton processes. Diagram (6) shows the contribution of one-exciton scattering on $V^{(3)}$, whereas diagram (7) has one- and two-exciton scattering contributing to the fifth-order response. Diagrams (8) and (9), representing population transfer, are obtained from diagrams (2) and (6) by inserting shaded area representing the irreducible part of the one-exciton population $\langle \hat{B}_i^{\dagger} \hat{B}_j \rangle^i$. It is useful to display the 2D response in the frequency domain by performing a double Fourier transform of the response function. Closed expressions for $R^{(3)}$ and $R^{(5)}$ for $V^{(3)} = 0$ are given in Appendix D.

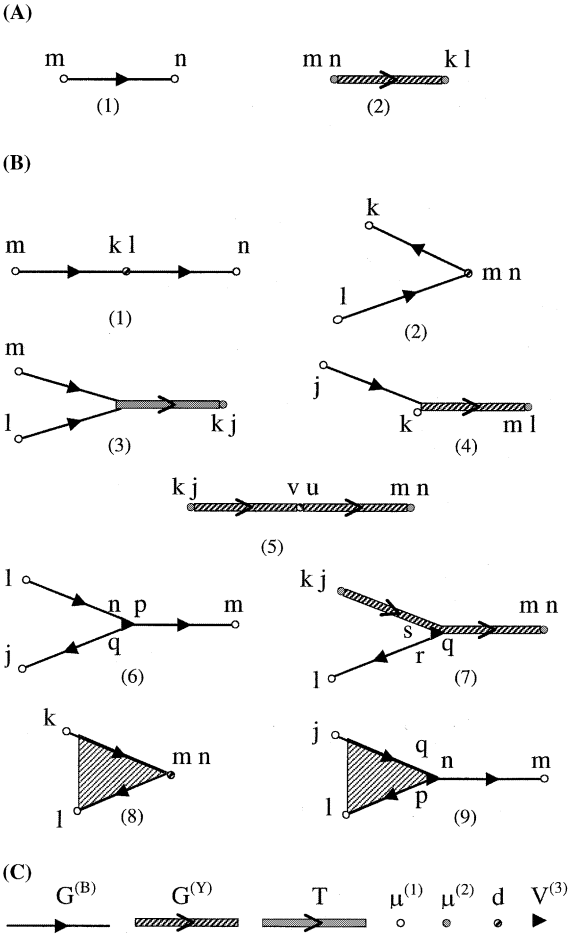

Fig. 2. Diagrammatic representation of (A) $R^{(3)}$ and (B) $R^{(5)}$. (C) Correspondence rules between the diagrammatic notations and actual quantities which they represent in Eqs. (2.28), (2.29), (B.1)–(B.7), (C.1), and (C.2). Arrows pointed to the right define forward time propagation. Arrows pointed to the left define backward time propagation and correspond to the hermitian conjugate quantities.

3. Discussion

The fifth-order response function (see Eqs. (2.31), (B.1)–(B.7), and (C.1) and (C.2)), obtained in this article, accounts for exciton scattering induced by the $V^{(3)}$ and $V^{(4)}$ anharmonicities.

The exciton–exciton scattering due to $V^{(4)}$ conserves number of vibrational quanta. The exciton scattering matrix entering the response function accounts for multiple exciton scattering processes to all orders of perturbation theory [37]. According to this, the quartic anharmonicity in the response function needs not necessarily be weak compared to the vibrational frequency differences. The present equations are similar to the NEE [39] but differ in some important technical details: First the cubic nonlinearity $V^{(3)}$ which was neglected in the NEE is included here perturbatively. Second, our creation and annihilation operators satisfy the Bose statistics (Eq. (2.5)). In the NEE we used non-Boson operators where the commutation relations Eq. (2.5) have an additional term in the right-hand side [38,39]. When the ratio κ between the 1–2 and 0–1 vibrational transition dipoles is equal $\sqrt{2}$ (as in the harmonic oscillator) they become Bosonic. There is a freedom in choosing the operators and incorporating exciton couplings either in anharmonicities or in the statistics. This

freedom may be used to simplify the analysis in different applications.

In contrast to $V^{(4)}$, the contribution of $V^{(3)}$ to the fifth-order response (see Eqs. (B.6), (B.7), and (C.2)) is assumed to be weak and is taken into account perturbatively. If $V^{(4)}=0$ then the only terms $R_1^{(5)}$, $R_2^{(5)}$, and $R_6^{(5)}$ (Eqs. (B.1), (B.2), and (B.6), respectively) contribute to the coherent signal. These terms coincide with Eqs. (4.4)–(4.6) for the response function, obtained in Ref. [31], with the correlation function taken in the form given by Eq. (5.9) in the same reference. These expressions represent classical contribution to the fifth-order response function for weak anharmonicities. Quantum corrections to $R_1^{(5)}$, $R_2^{(5)}$, and $R_6^{(5)}$ to high order in $V^{(3)}$ can be calculated in the same way as in Ref. [31]. For $V^{(4)}=0$ and a single anharmonic vibration, the incoherent contribution to the signal given by $R_8^{(5)}$ and $R_9^{(5)}$ (see Eqs. (C.1) and (C.2)) coincides with the semiclassical expressions given by Eq. (11) in Ref. [27].

Structure determination depends on the sensitivity of the fifth-order response function on the coupling between chromophores. To demonstrate how the cross-peak intensities depend on Coulomb coupling $J_{m,n}^{(e)}$ between the localized electronic states, we consider a system of N chromophores and assume that each electronic transition frequency and electronic transition dipole depends only on one localized vibrational coordinate, i.e. $\Omega^{(e)}(q_n)$ and $d^{(e)}(q_n)$, $n=1,\ldots,N$. Expanding the off-resonant electronic polarizability to first order in $J_{mn}^{(e)}$ we obtain

$$\alpha(\omega,q)=\sum_{mn}\left[\delta_{m,n}\frac{|d^{(e)}(q_m)|^2}{\omega-\Omega^{(e)}(q_m)}+(1-\delta_{m,n})\times J_{mn}\frac{d^{(e)}(q_m)d^{(e)}(q_n)}{[\omega-\Omega^{(e)}(q_m)][\omega-\Omega^{(e)}(q_n)]}\right], \tag{3.1}$$

where ω is the optical frequency. According to Eq. (3.1), for $m\neq n$, d_{mn}, $\mu_{mn}^{(2)}\sim\partial^2(\alpha(\omega,q))/\partial q_m\partial q_n\sim J_{mn}^{(e)}$. This means that the cross-peaks associated with response function components (see Eqs. (B.1)–(B.7)) consisting of d_{mn} and $\mu_{mn}^{(2)}$ are proportional to $J_{mn}^{(e)}$.

Currently, third-order nonlinear IR techniques and their applications to study vibrational dynamics of the amide I band in proteins and polypeptides are the focus of numerous experimental and theoretical studies [43–45,47–52]. In general these are 3D techniques. When one of the delay times set to zero, four coherent 2D techniques: photon echo, reverse photon echo, transient gratings and reverse transient gratings are possible [39]. The Raman counterpart of these techniques should be described by the seventh order response function. This can be calculated for vibrational excitons by extending the expressions derived in this article.

Acknowledgements

The support of the National Science Foundation and the Petroleum Research Fund administered by the American Chemical Society is gratefully acknowledged.

Appendix A. The fifth-order response for vanishing cubic anharmonicities

Solution of Eqs. (2.16)–(2.19) with $V^{(3)}=0$ gives the following terms contributing to the fifth-order response:

$$R_1(t;\tau_2,\tau_1)=\sum\mu_m^{(1)}\mu_n^{(1)^*}d_{kl}\times G_{mk}^{(B_0)}(t-\tau_2)G_{ln}^{(B_0)}(\tau_2-\tau_1), \tag{A.1}$$

$$R_2(t;\tau_2,\tau_1)=\sum d_{mn}\mu_k^{(1)^*}\mu_l^{(1)}\times[G_{nk}^{(B_0)}(t-\tau_1)G_{lm}^{(B_0)\dagger}(t-\tau_2)+G_{nk}^{(B_0)}(t-\tau_2)G_{lm}^{(B_0)\dagger}(t-\tau_1)], \tag{A.2}$$

$$R_3(t;\tau_2,\tau_1)=\int_{\tau_2}^{t}\mathrm{d}\tau'\sum\mu_m^{(1)}\mu_{kj}^{(2)^*}\mu_l^{(1)}G_{ms}^{(B_0)}(t-\tau')\times[G_{lr}^{(B_0)\dagger}(\tau'-\tau_2)T_{rs,kj}^{(R)}(\tau'-\tau_1)+G_{lr}^{(B_0)\dagger}(\tau'-\tau_1)T_{rs,kj}^{(R)}(\tau'-\tau_2)], \tag{A.3}$$

$$R_4(t;\tau_2,\tau_1) = 2\int_{\tau_2}^{t} \mathrm{d}\tau' \sum \mu^{(2)}_{mn}\mu^{(1)^*}_{k}\mu^{(1)^*}_{j} \times T^{(L)}_{mn,rs}(t-\tau')G^{(B_0)}_{sk}(\tau'-\tau_1) \times G^{(B_0)}_{rj}(\tau'-\tau_2), \quad (A.4)$$

$$R_5(t;\tau_2,\tau_1) = 2\int_{\tau_2}^{t} \mathrm{d}\tau'' \int_{\tau_1}^{\tau_2} \mathrm{d}\tau' \sum \mu^{(2)}_{mn} d_{vu} \mu^{(2)^*}_{kj} \times T^{(L)}_{mn,rs}(t-\tau'')G^{(B_0)}_{sv}(\tau''-\tau_2)G^{(B_0)}_{uq} \times (\tau_2-\tau')G^{(B_0)}_{rp}(\tau''-\tau')T^{(R)}_{pq,jk}(\tau'-\tau_1). \quad (A.5)$$

We have introduced the auxiliary quantities

$$T^{(R)}_{mn,kj}(t) \equiv \int_0^t \mathrm{d}\tau \bar{\Gamma}^{(i)}_{mn,rs}(t-\tau)G^{(B_0)}_{rk}(\tau)G^{(B_0)}_{sj}(\tau), \quad (A.6)$$

$$T^{(L)}_{mn,kj}(t) \equiv \int_0^t \mathrm{d}\tau G^{(B_0)}_{mr}(\tau)G^{(B_0)}_{ns}(\tau)\bar{\Gamma}^{(i)}_{rs,kj}(t-\tau), \quad (A.7)$$

where $\bar{\Gamma}^{(i)}_{mn,kj}(t)$ is the irreducible part of the scattering matrix obtained by subtracting the local-field part from $\bar{\Gamma}_{mn,kj}(t)$:

$$\bar{\Gamma}^{(i)}_{mn,kj}(t) \equiv \bar{\Gamma}_{mn,kj}(t) - \mathrm{i}\delta'(t)\delta_{mk}\delta_{nj} - \delta(t)(h_{mk}\delta_{nj} + \delta_{mk}h_{nj}). \quad (A.8)$$

Appendix B. The fifth-order response function with cubic and quartic anharmonicity

In this appendix we represent coherent fifth-order response associated with both cubic and quartic anharmonicities. Solving Eqs. (2.16)–(2.19) and retaining only first-order contributions in the perturbative expansion of the response function in powers of $V^{(3)}$, one obtains:

$$R^{(5)}_1(t;\tau_2,\tau_1) = \sum \mu^{(1)}_m d_{kl}\mu^{(1)^*}_n \times G^{(B)}_{mk}(t-\tau_2)G^{(B)}_{ln}(\tau_2-\tau_1), \quad (B.1)$$

$$R^{(5)}_2(t;\tau_2,\tau_1) = -\sum_{mn} d_{mn}\mu^{(1)}_l\mu^{(1)^*}_k \times [G^{(B)}_{nk}(t-\tau_1)G^{(B)^\dagger}_{lm}(t-\tau_2) + G^{(B)}_{nk}(t-\tau_2)G^{(B)^\dagger}_{lm}(t-\tau_1)], \quad (B.2)$$

$$R^{(5)}_3(t;\tau_2,\tau_1) = -\sum \mu^{(1)}_m\mu^{(1)}_l\mu^{(2)^*}_{kj} \int_{\tau_2}^{t} \mathrm{d}\tau' G^{(B)}_{ms}(t-\tau') \times [G^{(B)^\dagger}_{lr}(\tau'-\tau_2)T_{rs,kj}(\tau'-\tau_1) + G^{(B)^\dagger}_{lr}(\tau'-\tau_1)T_{rs,kj}(\tau'-\tau_2)], \quad (B.3)$$

$$R^{(5)}_4(t;\tau_2,\tau_1) = 2\sum \mu^{(2)}_{mn}\mu^{(1)^*}_k\mu^{(1)^*}_j \times G^{(Y)}_{mn,kl}(t-\tau_2)G^{(B)}_{lj}(\tau_2-\tau_1), \quad (B.4)$$

$$R^{(5)}_5(t;\tau_2,\tau_1) = 2\sum \mu^{(2)}_{mn}d_{vu}\mu^{(2)^*}_{kj} \times G^{(Y)}_{mnvq}(t-\tau_2)G^{(Y)}_{uqkj}(\tau_2-\tau_1), \quad (B.5)$$

$$R^{(5)}_6(t;\tau_2,\tau_1) = \mathrm{i}\sum \mu^{(1)}_m\mu^{(1)}_l\mu^{(1)^*}_j V^{(3)}_{npq} \int_{\tau_2}^{t} \mathrm{d}\tau' G^{(B)}_{mn}(t-\tau') \times [G^{(B)^\dagger}_{pl}(\tau'-\tau_1)G^{(B)}_{qj}(\tau'-\tau_2) + G^{(B)^\dagger}_{pl}(\tau'-\tau_2)G^{(B)}_{qj}(\tau'-\tau_1)], \quad (B.6)$$

$$R^{(5)}_7(t;\tau_2,\tau_1) = 4\mathrm{i}\sum \mu^{(2)}_{mn}\mu^{(1)}_l\mu^{(1)^*}_{kj} V^{(3)}_{qrs} \times \int_{\tau_2}^{t} \mathrm{d}\tau' G^{(Y)}_{mnpq}(t-\tau') \times [G^{(B)^\dagger}_{rl}(\tau'-\tau_1)G^{(Y)}_{ps,kj}(\tau'-\tau_2) + G^{(B)^\dagger}_{rl}(\tau'-\tau_2)G^{(Y)}_{ps,kj}(\tau'-\tau_1)]. \quad (B.7)$$

In Eq. (B.3) we use auxiliary function

$$T_{mn,pq}(t) = \int_0^t \mathrm{d}\tau \bar{\Gamma}_{mn,rs}(t-\tau)F^{(Y)}_{rs,pq}(\tau) \quad (B.8)$$

where $\bar{F}^{(Y)}$ represents the two-exciton Green function of Eqs. (2.17) and (2.19) with $V^{(4)} = 0$, satisfying the Bethe–Salpeter equation

$$F^{(Y)}_{mn,pq}(t) = G^{(B_0)}_{mp}(t)G^{(B_0)}_{nq}(t) + \sum \int \mathrm{d}\tau' \times \int \mathrm{d}\tau'' G^{(B_0)}_{mn}(t-\tau)G^{(B_0)}_{ns}U^{\mathrm{eff}}_{rs,kl} \times (\tau'-\tau'')F^{(Y)}_{kl,pq}(\tau''). \quad (B.9)$$

Appendix C. Exciton relaxation and transport

Vibrational relaxation processes can be included by adding harmonic bath degrees of free-

dom to the Hamiltonian equation (2.6). We assume linear coupling $\sum \bar{h}_{mn;j}\hat{B}_m^\dagger \hat{B}_n q_j$ between the bath coordinates $\{q_j\}$ and exciton degrees of freedom characterized by the coupling constant $\bar{h}_{mn;j}$. This corresponds to the bath-induced self-energy in the expression for $G_{mn}^{(B_0)}(t)$ used in Eqs. (2.20), (2.22), (2.23), and (2.25) [38]. The real part of the bath-induced self-energy renormalizes the vibrational frequencies and may be included in Ω_n. The imaginary part is included by introducing dephasing rate $\hat{\Gamma}$. We take the simplest relaxation model introducing dephasing rate matrix elements in the form $[\hat{\Gamma}]_{mn} = \Gamma\delta_{mn}$. Coupling to the collective bath coordinates also induces dephasing and population relaxation processes within one-exciton manifold described by the irreducible part of the exciton population $\langle B_i^\dagger B_j\rangle^i$ whose contribution to the response function was neglected in Section 2. This part gives rise to additional incoherent components of the optical response

$$R_8^{(5)}(t;\tau_2,\tau_1) = -\sum d_{mn}\mu_k^{(1)^*}\mu_l^{(1)}\bar{G}_{mn,k'l'}(t-\tau_2) \times \Big[\delta_{l'l}G_{k'k}^{(B)}(\tau_2-\tau_1) - \delta_{kk'}G_{ll'}^{(B)\dagger}(\tau_2-\tau_1)\Big], \tag{C.1}$$

$$R_9^{(5)}(t;\tau_2,\tau_1) = -3\mathrm{i}\sum \mu_m^{(1)}\mu_l^{(1)}\mu_j^{(1)^*}V_{npq}^{(3)} \times \int_{\tau_2}^{t} \mathrm{d}\tau' G_{mn}^{(B)}(t-\tau') \times \bar{G}_{pq,p'q'}(\tau'-\tau_2)\Big[\delta_{pl}G_{qj}^{(B)}(\tau_2-\tau_1) - G_{pl}^{(B)\dagger}(\tau_2-\tau_1)\delta_{qj}\Big], \tag{C.2}$$

where $\bar{G}_{mn,k'l'}(t)$ is the incoherent part of the Green function satisfying the Redfield equation which describe the time evolution of $\langle B_i^\dagger B_j\rangle^i$ [38].

Appendix D. 2D response function in the frequency domain using the exciton basis set

In this appendix we calculate the third and the fifth-order response function in the frequency domain, assuming $V^{(3)} = 0$.

We adopt the exciton basis set

$$|\Psi_\alpha\rangle = \sum_n \psi_\alpha(n)\hat{B}_n^\dagger|0\rangle, \tag{D.1}$$

where $|0\rangle$ is the exciton vacuum state as well as ω_α and $\psi_\alpha(n)$ are one-exciton energies and wavefunctions satisfying the equation

$$\sum_n (h_{mn} - \delta_{mn}\omega_\alpha)\psi_\alpha(n) = 0 \tag{D.2}$$

with the Hamiltonian h_{mn} given by Eqs. (2.6) and (2.7). In the exciton representation the one-particle Green function is

$$G_{mn}(t) = \theta(t)\sum_\alpha \psi_\alpha(m)\psi_\alpha^*(n)\exp(-\mathrm{i}\omega_\alpha t - \Gamma t). \tag{D.3}$$

The third-order response function has two components given by Eqs. (2.28) and (2.29). To calculate $R_1^{(3)}$ we substitute Eq. (D.3) into Eq. (2.28). By performing the Fourier transformation

$$R^{(3)}(\Omega_1) = \int_0^\infty \mathrm{d}t_1 \mathrm{e}^{\mathrm{i}\Omega_1 t_1}R^{(3)}(t_1), \tag{D.4}$$

where $t_1 = t - \tau_1$, we obtain

$$R_1^{(3)}(\Omega_1) = \sum_\alpha \frac{|\mu_\alpha^{(1)}|^2}{\Omega_1 - \omega_\alpha + \mathrm{i}\Gamma}, \tag{D.5}$$

with

$$\mu_\alpha^{(1)} = \sum_n \mu_n^{(1)}\psi_\alpha(n). \tag{D.6}$$

To calculate $R_2^{(3)}$, we substitute Eq. (D.3) into Eq. (2.23), and the resulting expression into Eq. (2.22). By setting $V^{(3)} = 0$ in Eqs. (2.24) and (2.25) and using Eq. (2.22) we find two-exciton Green function. By performing the Fourier transform Eq. (D.4) of two-exciton Green function we find

$$R_2^{(3)}(\Omega_1) = \sum_{\alpha,\beta,\gamma,\delta} \mu_{\alpha\beta}^{(2)}\mu_{\gamma\delta}^{(2)^*}F_{\alpha\beta}^{(Y_0)}(\Omega_1) \times [1 - F^{(Y_0)}(\Omega_1)V^{(4)}]^{-1}_{\alpha\beta,\gamma\delta}, \tag{D.7}$$

where

$$V_{\alpha\beta,\gamma\delta}^{(4)} = \sum_{mnls} \psi_\alpha^*(m)\psi_\beta^*(n)V_{mnls}^{(4)}(\omega)\psi_\gamma(l)\psi_\delta(s), \tag{D.8}$$

$$F^{(Y_0)}_{\alpha\beta}(\omega) = \frac{1}{\omega - (\omega_\alpha + \omega_\beta) + 2i\Gamma}. \tag{D.9}$$

According to Eqs. (D.5) and (D.7) third-order response function has resonances at one-exciton energies ω_α and at two-exciton energies $\bar{\omega}_\nu$, the later are determined by the poles of the right-hand side of Eq. (D.7).

To calculate the fifth-order response, we substitute Eq. (D.3) into Eqs. (A.1)–(A.7) and perform 2D Fourier transformation of the response function

$$R^{(5)}(\Omega_2, \Omega_1) = \int_0^\infty dt_2 \int_0^\infty dt_1 e^{i\Omega_1 t_1 + i\Omega_2 t_2} R^{(5)}(t_2, t_1), \tag{D.10}$$

where $t_1 = \tau_2 - \tau_1$ and $t_2 = t - \tau_2$ (Fig. 1). This gives the frequency domain representation for the optical response:

$$R^{(5)}_1(\Omega_2,\Omega_1) = \sum \mu^{(1)}_\alpha \mu^{(1)^*}_\beta d_{\alpha\beta} \times \frac{1}{[\Omega_1 - \omega_\beta + i\Gamma][\Omega_2 - \omega_\alpha + i\Gamma]} + \text{c.c.}, \tag{D.11}$$

$$R^{(5)}_2(\Omega_2, \Omega_1) = \sum \mu^{(1)^*}_\alpha \mu^{(1)}_\beta d_{\beta\alpha} \times \left[\frac{1}{[\Omega_1 - \omega_\alpha + i\Gamma][\Omega_2 - (\omega_\alpha - \omega_\beta) + 2i\Gamma]} + \frac{1}{[\Omega_2 + \omega_\beta + i\Gamma][\Omega_1 - (\omega_\alpha - \omega_\beta) + 2i\Gamma]} \right] + \text{c.c.}, \tag{D.12}$$

$$R^{(5)}_3(\Omega_2, \Omega_1) = i^4 \sum \mu^{(1)}_\alpha \mu^{(1)}_\beta \mu^{(2)^*}_{\gamma\delta} \times \left[\frac{\bar{\Gamma}^{(i)}_{\alpha\beta,\gamma\delta}(\Omega_1)}{[\Omega_2 - \Omega_1 + \omega_\beta + i\Gamma][\Omega_1 - (\omega_\gamma + \omega_\delta) + 2i\Gamma]} + \frac{\bar{\Gamma}^{(i)}_{\alpha\beta,\gamma\delta}(\Omega_2 + \omega_\beta + i\Gamma)}{[\Omega_1 - \omega_\alpha + i\Gamma][\Omega_2 - (\omega_\gamma + \omega_\delta - \omega_\beta) + 3i\Gamma]} \right] + \text{c.c.}, \tag{D.13}$$

$$R^{(5)}_4(\Omega_2, \Omega_1) = 2 \sum \mu^{(2)}_{\gamma\delta} \mu^{(1)^*}_\alpha \mu^{(1)^*}_\beta \times \frac{1}{[\Omega_1 - \omega_\alpha + i\Gamma]} \times \frac{\bar{\Gamma}^{(i)}_{\gamma\delta,\alpha\beta}(\Omega_2)}{[\Omega_2 - (\omega_\gamma + \omega_\delta) + 2i\Gamma][\Omega_2 - (\omega_\alpha + \omega_\beta) + 2i\Gamma]} + \text{c.c.}, \tag{D.14}$$

$$R^{(5)}_5(\Omega_2, \Omega_1) = -2i \sum \mu^{(2)}_{\delta\sigma} d_{\beta\gamma} \mu^{(2)^*}_{\xi\zeta} \times \frac{\bar{\Gamma}^{(i)}_{\delta\sigma,\beta\alpha}(\Omega_2)}{[\Omega_2 + (\omega_\delta + \omega_\sigma) + 2i\Gamma][\Omega_2 - (\omega_\alpha + \omega_\beta) + 2i\Gamma]} \times \frac{\bar{\Gamma}^{(i)}_{\gamma\alpha,\xi\zeta}(\Omega_1)}{[\Omega_1 - (\omega_\gamma + \omega_\alpha) - 2i\Gamma][\Omega_1 - (\omega_\xi + \omega_\zeta) + 2i\Gamma]} + \text{c.c.}, \tag{D.15}$$

where

$$\mu^{(2)}_{\alpha\beta} = \sum_{nm} \psi^*_\alpha(n) \mu^{(2)}_{nm} \psi_\beta(m), \tag{D.16}$$

$$d_{\alpha\beta} = \sum_{nm} \psi^*_\alpha(n) d_{nm} \psi_\beta(m), \tag{D.17}$$

$$\bar{\Gamma}^{(i)}_{\alpha\beta,\gamma\delta}(\omega) = \sum_{mnls} \psi^*_\alpha(m) \psi^*_\beta(n) \bar{\Gamma}^{(i)}_{mn,ls}(\omega) \psi_\gamma(l) \psi_\delta(s). \tag{D.18}$$

$\bar{\Gamma}^{(i)}_{mn,ls}(\omega)$ is the Fourier transform of the time domain irreducible part of scattering matrix defined by Eq. (A.8). By solving Eqs. (A.8) and (2.23) in the frequency domain and in the exciton bases set (Eqs. (D.1) and (D.2)) we obtain the expression for the irreducible part of the scattering matrix:

$$\bar{\Gamma}^{(i)}_{\alpha\beta,\gamma\delta}(\omega) = \left[1 - V^{(4)} F^{(Y_0)}(\omega)\right]^{-1}_{\alpha\beta,\gamma\delta} \times (\omega - (\omega_\gamma + \omega_\delta) + 2i\Gamma). \tag{D.19}$$

Signal components determined by $R^{(5)}_1$ and $R^{(5)}_2$ represent various correlations between the one-exciton states which show up as $(\omega_\alpha, \omega_\beta)$ and $(\omega_\alpha, \omega_\alpha - \omega_\beta)$ 2D resonances, respectively. Components $R^{(5)}_3$ and $R^{(5)}_4$ describe various correlations between one- and two-exciton states. $R^{(5)}_3$ is resonant at $(\bar{\omega}_\alpha, \bar{\omega}_\alpha - \omega_\beta)$ and $(\omega_\alpha, \bar{\omega}_\beta - \omega_\gamma)$, whereas $R^{(5)}_4$ has only $(\omega_\alpha, \bar{\omega}_\beta)$ resonances. The last term

$R_5^{(5)}$ is due to the correlations between the two-exciton states only and has resonances at $(\bar{\omega}_\alpha, \bar{\omega}_\beta)$.

Finally we present the incoherent contribution to the optical signal (Eq. (C.1)) in the frequency domain using exciton representation

$$R_6^{(5)}(\Omega_2,\Omega_1) = \sum d_{\alpha\beta}\mu_\gamma^{(1)^*}\mu_\delta^{(1)}\bar{G}_{\alpha\beta,\gamma\delta}(\Omega_1) \times \frac{\omega_\delta+\omega_\gamma-2i\Gamma}{[\Omega_2-\omega_\gamma+i\Gamma][\Omega_2+\omega_\delta-i\Gamma]}, \tag{D.20}$$

where

$$\bar{G}_{\alpha\beta,\gamma\delta}(\omega) = \sum_{mnkl}\psi_\alpha(m)\psi_\beta^*(n)\bar{G}_{mn,kl}(\omega)\psi_\gamma(k)\psi_\delta^*(l) \tag{D.21}$$

$\bar{G}_{mn,kl}(\omega)$ is Fourier transform of the incoherent part Green function entering Eq. (C.1).

References

[1] R.R. Ernst, G. Bodenhausen, A. Wokaun, Principles of Nuclear Magnetic Resonance in One and Two-Dimensions, Clarendon Press, Oxford, 1987.
[2] J.N. Evans, Biomolecular NMR Spectroscopy, Oxford University Press, New York, 1995.
[3] J.K.M. Sanders, B.H. Hunter, Modern NMR Spectroscopy, Oxford University Press, New York, 1993.
[4] S. Mukamel, Principles of Nonlinear Optical Spectroscopy, Oxford University Press, New York, 1995.
[5] Y. Tanimura, S. Mukamel, J. Chem. Phys. 99 (1993) 9496.
[6] T. Steffen, K. Duppen, Chem. Phys. Lett. 290 (1998) 229.
[7] T. Steffen, K. Duppen, Phys. Rev. Lett. 76 (1996) 1224.
[8] T. Steffen, J.T. Fourkas, K. Duppen, J. Chem. Phys. 105 (1996) 7364.
[9] D. Blank, L. Kaufman, G. Fleming, J. Chem. Phys. 113 (2000) 771.
[10] D. Blank, L. Kaufman, G. Fleming, J. Chem. Phys. 111 (1999) 3105.
[11] A. Tokmakoff, M.J. Lang, D.S. Larsen, G.R. Fleming, V. Chernyak, S. Mukamel, Phys. Rev. Lett. 79 (1997) 2702.
[12] A. Tokmakoff, G.R. Fleming, J. Chem. Phys. 106 (1997) 2569.
[13] A. Tokmakoff, M.J. Lang, D.S. Larsen, G.R. Fleming, Chem. Phys. Lett. 272 (1997) 48.
[14] J.C. Kirkwood, A.C. Albrecht, D.J. Ulness, J. Chem. Phys. 111 (1999) 253.
[15] J.C. Kirkwood, A.C. Albrecht, D.J. Ulness, M.J. Stimson, J. Chem. Phys. 111 (1999) 272.
[16] K. Tominaga, K. Yoshihara, J. Chem. Phys. 104 (1996) 4419.
[17] K. Tominaga, K. Yoshihara, J. Chem. Phys. 104 (1996) 1159.
[18] K. Tominaga, G.P. Keogh, Y. Naitoh, K. Yoshihara, J. Raman Spectrosc. 26 (1995) 495.
[19] K. Tominaga, K. Yoshihara, Phys. Rev. Lett. 74 (1995) 3061.
[20] M. Cho, K. Okumura, Y. Tanimura, J. Chem. Phys. 108 (1998) 1326.
[21] K. Okumura, Y. Tanimura, J. Chem. Phys. 107 (1997) 2267.
[22] K. Okumura, Y. Tanimura, J. Chem. Phys. 106 (1997) 1687.
[23] M. Berg, D.A.V. Bout, Acc. Chem. Res. 30 (1997) 65.
[24] S.P. Palese, J.T. Buontempo, L. Schilling, W.T. Lotshaw, Y. Tanimura, S. Mukamel, R.J.D. Miller, J. Phys. Chem. 98 (1994) 12466.
[25] K. Okumura, A. Tokmakoff, Y. Tanimura, J. Chem. Phys. 111 (1999) 492.
[26] T. Steffen, K. Duppen, J. Chem. Phys. 106 (1997) 3854.
[27] V. Chernyak, A. Piryatinski, S. Mukamel, Laser Chem. 19 (1999) 109.
[28] R.W. Hellwarth, Third-order optical susceptibilities of liquids and solids, Progr. Quant. Electron. 5 (1977) 2.
[29] V. Khidekel, S. Mukamel, Chem. Phys. Lett. 240 (1995) 304.
[30] S. Mukamel, V. Khidekel, V. Chernyak, Phys. Rev. E 53 (1996) R1.
[31] V. Chernyak, S. Mukamel, J. Chem. Phys. 108 (1998) 5812.
[32] S. Mukamel, A. Piryatinski, V. Chernyak, Acc. Chem. Res. 32 (1999) 145.
[33] S. Mukamel, Ann. Rev. Phys. Chem. 51 (2000) 691.
[34] S. Mukamel, A. Piryatinski, V. Chernyak, J. Chem. Phys. 110 (1999) 1711.
[35] R.B. Williams, R.F. Loring, J. Chem. Phys. 113 (2000) 1931.
[36] S. Saito, I. Ohmine, J. Chem. Phys. 108 (1998) 240.
[37] V. Chernyak, N. Wang, S. Mukamel, Phys. Rep. 263 (1995) 213.
[38] V. Chernyak, W.M. Zhang, S. Mukamel, J. Chem. Phys. 109 (1998) 9587.
[39] W.M. Zhang, V. Chernyak, S. Mukamel, J. Chem. Phys. 110 (1999) 5011.
[40] T.E. Creighton, Proteins: Structure and Molecular Properties, second ed., W.H. Freeman, New York, 1993.
[41] S. Krimm, J. Bandeker, J. Adv. Protein Chem. 38 (1986) 181.
[42] H. Torii, M. Tasumi, J. Chem. Phys. 96 (1992) 3379.
[43] P. Hamm, M. Lim, R.M. Hochstrasser, J. Phys. Chem. B 102 (1998) 6123.
[44] A. Piryatinski, S. Tretiak, V. Chernyak, S. Mukamel, J. Raman Spectrosc. 31 (2000) 125.
[45] A. Piryatinski, V. Chernyak, S. Mukamel, in: M.D. Fayer (Ed.), Ultrafast Infrared and Raman Spectroscopy, Marcel Dekker, New York, 2001, pp. 349–383.

[46] V. Chernyak, S. Mukamel, J. Opt. Soc. Am. B 13 (1996) 1302.
[47] P. Hamm, M. Lim, W.F. DeGrado, R. Hochstrasser, Proc. Natl. Acad. Sci. USA 96 (1999) 2036.
[48] P. Hamm, M. Lim, W.F. DeGrado, R. Hochstrasser, J. Chem. Phys. 112 (2000) 1907.
[49] S. Woutersen, P. Hamm, J. Phys. Chem. 104 (2000) 11316.
[50] C. Scheurer, A. Piryatinski, S. Mukamel, in: T. Elsasser, S. Mukamel, M. Murnane, N.F. Scherer (Eds.), Ultrafast Phenomena XII, Springer Series in Chemical Physics, Springer, Berlin, 2000, p. 50.
[51] C. Scheurer, A. Piryatinski, S. Mukamel, J. Am. Chem. Soc. in press.
[52] M.C. Asplund, M.T. Zanni, R. Hochstrasser, Proc. Natl. Acad. Sci. USA 97 (2000) 219.